Supporting Information for:

Promoting Morphology with a Favorable Density-of-States Using Diiodooctane to Improve Organic Photovoltaic Device Efficiency and Charge Carrier Lifetimes

Logan E. Garner,[†] Abhijit Bera,[‡] Bryon W. Larson,[†] David P. Ostrowski,[§] Amlan J. Pal,[‡,*] and Wade A. Braunecker[†,*]

[†] Chemistry & Nanoscience Center, National Renewable Energy Laboratory, Golden, Colorado 80401, United States

[‡] Department of Solid State Physics, Indian Association for the Cultivation of Science, Jadavpur, Kolkata 700032, India

[§] Department of Electrical, Computer and Energy Engineering, University of Colorado Boulder, Boulder, Colorado 80309, United States

Email: sspajp@iacs.res.in, Wade.Braunecker@nrel.gov

Table of Contents

I. General Experimental Details

All chemicals and solvents were purchased from commercial sources and used as received unless stated otherwise. PCE10 was purchased from 1-Material. $PC_{70}BM$ was purchased from Nano-C. Patterned ITO (Thin Films Devices, Inc.) and all quartz substrates (Allen Scientific Glass) were washed with Liquinox, sonicated sequentially in D.I. water, acetone, isopropyl alcohol, and UV-ozone treated for 30 minutes before use or device fabrication. Au (111) substrates were purchase from Phasis (Switzerland). Neat and active layer blend films for AFM, STS/STM, and TRMC analysis were spin cast inside a glove box under an inert N_2 atmosphere.

II. Device Preparation and Characterization

A diethyl zinc solution was prepared under nitrogen by combining 15% diethyl zinc in anhydrous toluene with anhydrous THF in a 1:4 ratio. Thin ZnO layers were deposited on patterned ITO substrates by spin coating 200 μL of the diethyl zinc solution in air using a spin speed of 5000 rpm, ramp rate of 5000 rpm/sec, and spin time of 30 sec. The substrate was then annealed (inside a glove box) at 120 °C for 20 min. Active layers were prepared entirely inside a glove box under inert atmosphere by first making PCE10 and $PC_{70}BM$ stock solutions at concentrations of 12 mg/mL and 40 mg/mL, respectively, in chlorobenzene and in chlorobenzene containing 3% 1,8-diiodooctane (by volume) and stirring these stock solutions at 60 °C and 400 rpm for 48 hrs to ensure polymer and fullerene are completely dissolved before preparing blend solutions. Blend solutions were prepared by combining PCE10 and $PC_{70}BM$ stock solutions in 1:1.5 ratio by volume. Active layers were spin cast by dropping 120 μL of 60 °C blend solution and immediately spinning at 800 rpm with 800 rpm/sec ramp rate for 60 sec. Active layers were not annealed but were allowed to dry inside glove box for several hours before deposition of MoO_3 and Ag top contact. The 10 nm MoO_3 hole transport layer was evaporated on top of the

active layer followed by evaporation of a 100 nm thick Ag top contact. Hole transport layers and Ag top contacts were evaporated using an Angstrom Engineering thermal evaporator with a base pressure below 3×10^{-8} Torr. All handling of devices following fabrication was done under inert atmosphere.

Device characterization was performed under illumination using a Newport Oriel Sol3A class AAA solar simulator, and J–V curves were measured under 1 sun illumination. Short circuit currents were corrected for spectral mismatch using the procedure of Shrotriya *et al*.[1] EQE measurements were performed using a Newport Oriel IQE200 system with lock-in detection.

III. Atomic Force Microscopy

Topographic and phase imaging was performed with an Asylum Research AFM (MFP-3D). Budget sensors (tapping mode, Tapp300Al-G) cantilevers were used in the imaging of these samples. The AFM is housed in an acoustic box and placed on a vibration isolation table.

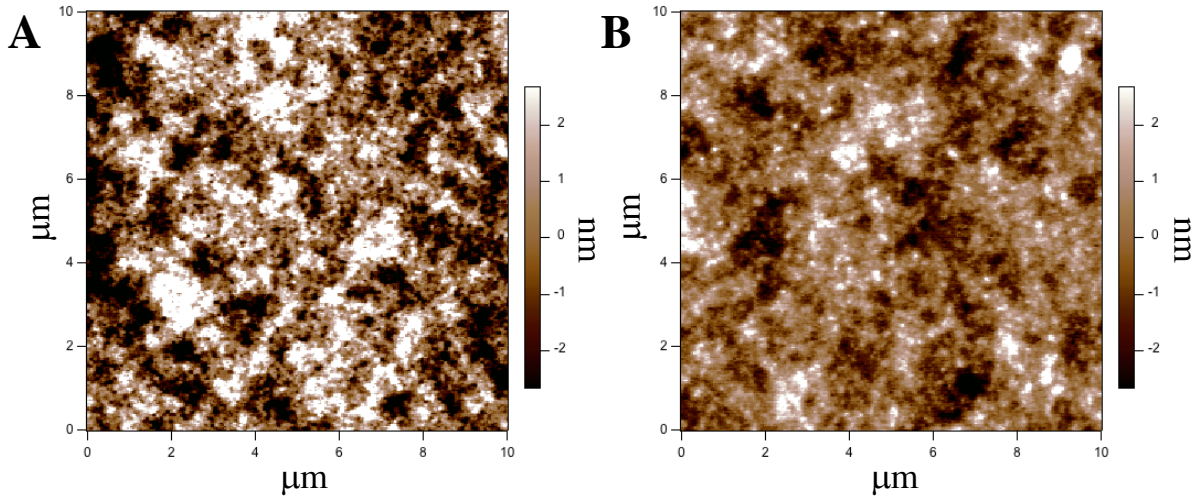

Figure S1. Atomic force microscopy topography images of (A) 100 nm thick 'DIO' active layer film prepared by the same conditions used for device preparation and (B) 10 nm thick 'DIO' active layer film prepared based upon conditions developed to prepare thin samples for STS/STM analysis with morphologies as similar as possible to their 100 nm thick counterparts. Other than differences in surface roughness (RMS_{100nm} = 2.0; RMS_{10nm} = 1.2), which is reasonable considering the differences in overall thickness as a result of different spin speeds to cast each film, the two active layer films appear to have similar morphologies. As such, the morphologies of the 10 nm thick films were deemed reasonable model samples for STM/STS analysis.

IV. Scanning Tunneling Spectroscopy / Microscopy

STM/STS sample preparation. Thin active layers with morphologies as close as possible to those of devices were prepared starting from stock solutions and active layer forming solutions identical to those employed for device fabrication. All preparation was performed under inert atmosphere. Upon mixing PCE10 and $PC_{70}BM$ stock solutions in volume ratio of 1:1.5 (to afford blend solutions with total dissolved solids concentrations of 28.8 mg/mL) these solutions were diluted by adding equivalent volumes of chlorobenzene (to no additive blend solution) and chlorobenzene containing 3% DIO (to DIO additive blend solution) resulting in solutions with

total dissolved solids concentrations of 14.4 mg/mL. Thin active layers were then prepared by dropping the solution onto Au (111) substrates and spinning at 6000 rpm with 6000 rpm/s ramp rate for 60 s. Upon completion of spinning active layers were allowed to dry under inert atmosphere for a minimum of 30 minutes. The films were quickly transferred from the glove-box to the load-lock chamber of STM followed by transfer to the main chamber for characterization.

STM/STS Analysis. STS measurements were performed at 80 K in an ultrahigh vacuum (2×10^{-10} Torr) condition. A RHK Pan style STM was used for this purpose in which both the tip and the film retained the same temperature. Tip-approach parameters were set to 2.0 V, 0.1 nA. Differential conductance measurements were performed through a standard lock-in technique with a modulation frequency of 971 Hz and rms voltage of 16 mV.

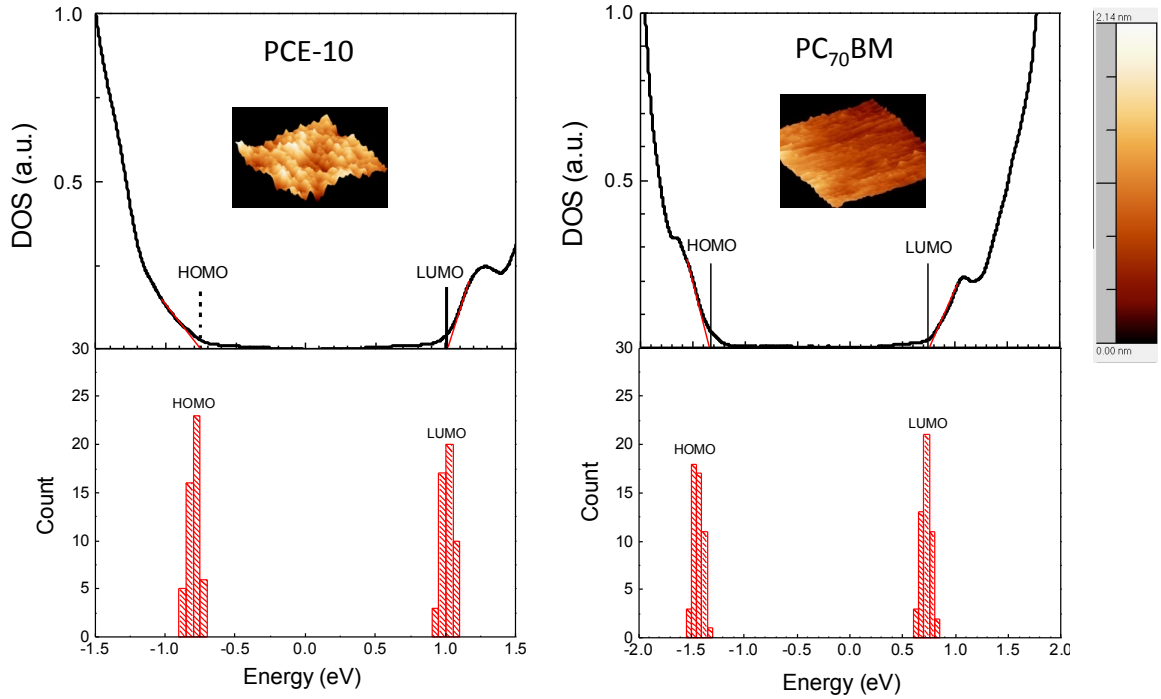

Figure S2. (Top) Numerical derivative of I–V characteristics versus tip-voltage plots for PCE-10 and $PC_{70}BM$ with marked HOMO and LUMO positions (100 nm × 100 nm topographic images in the inset); (bottom) histograms of the obtained HOMO and LUMO positions. PCE-10 transport gap: 1.7±0.1 eV. $PC_{70}BM$ transport gap: 2.15±0.1 eV.

Table S1. Summary of peak values and distributions of local DOS

Data set	Peak (eV)	Onset 1 (eV)	Onset 2 (eV)	Range Between Onsets (eV)	Half-width (eV)
Donor HOMO (neat)	-0.789	-0.879	-0.699	0.180	0.09
Donor HOMO (No additive)	-0.729	-0.946	-0.519	0.427	0.20
Donor HOMO (DIO additive)	-0.774	-1.028	-0.512	0.516	0.24
Acceptor LUMO (neat)	0.726	0.636	0.824	0.188	0.08
Acceptor LUMO (No additive)	0.749	0.479	1.026	0.547	0.26
Acceptor LUMO (DIO additive)	0.741	0.419	1.063	0.644	0.32

V. Time-Resolved Microwave Conductivity

TRMC is a pump-probe technique that can be used to measure the photoconductance of a film without the need for charge collection at electrical contacts.[2-3] The details of the experimental methodology have been presented elsewhere.[3-4] In brief, the sample is placed in a microwave cavity at the end of an X-band waveguide operating at ca. 9 GHz, and is photoexcited through a grid with a 5 ns laser pulse from an OPO pumped by the third harmonic of an Nd:YAG laser. The relative change of the microwave power, P, in the cavity, due to abrorption of the microwaves by the photoinduced free electrons and holes, is related to the transient photoconductance, ΔG, by $\Delta P/P = -K\Delta G$, where the calibration factor K is experimentally determined individually for each sample. Taking into account that the electrons and holes are generated in pairs, the peak photoconductance during the laser pulse can be expressed as[3]

$$\Delta G = \beta q_e F_A I_0 (\phi \cdot \Sigma\mu) \quad \textbf{(1)}$$

where q_e is the elementary charge, $\beta = 2.2$ is the geometric factor for the X-band waveguide used, I_0 is the incident photon flux, F_A the fraction of light absorbed at the excitation wavelength, ϕ is the quantum efficiency of free carrier generation per photon absorbed and $\Sigma\mu$ the sum of the mobilities of electrons and holes.[3] Eq. 1 is used to evaluate the quantum

efficiency or free carrier generation per photon absorbed, multiplied by the local mobility of free carriers. These quantities can often be correlated with molecular structure to provide insight into the mechanisms for free carrier generation and transport in polymer-fullerene composites as a function of the microstructure. The photoconductance decay after the end of the laser pulse is also a useful tool for the characterization of free carrier decay mechanisms by recombination and trapping. Active layer blend samples for this work were prepared on quartz substrates according to an optimized literature procedure.[5]

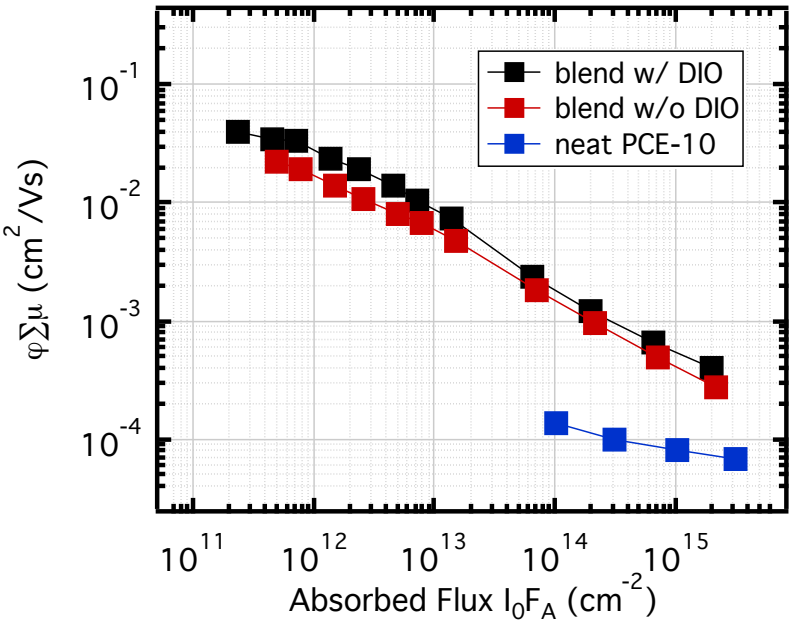

Figure S3. The product of charge carrier yield (ϕ) and sum of hole and electron mobilities ($\Sigma\mu$) is illustrated over a range of intensities spanning four orders of magnitude at a laser excitation intensity of 640 nm for neat PCE-10 donor polymer (blue) and blends of PCE-10 with $PC_{70}BM$ (1:1.5 ratio) both with (black) and without (red) DIO additive.

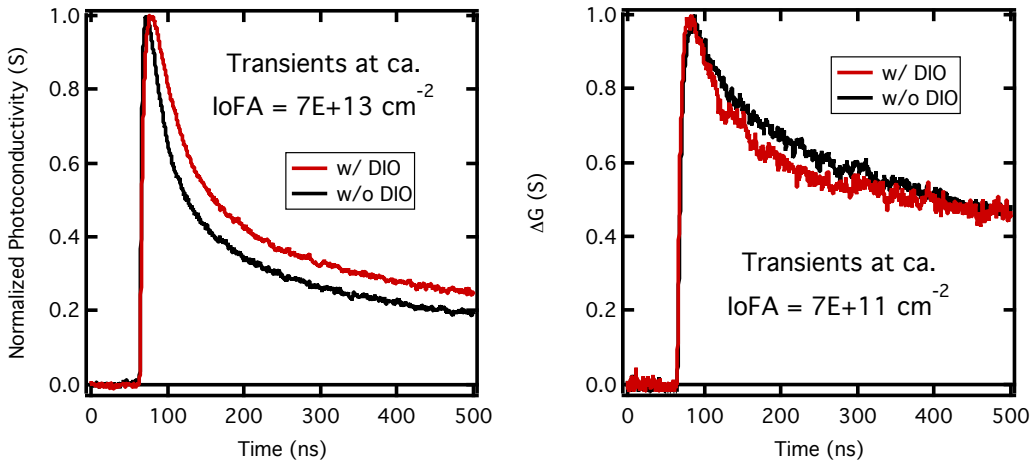

Figure S4. Normalized photoconductivity transients are shown for the "intermediate" (left, with IoFA = ~ 7e13 cm^{-2}) and "low" (right, with IoFA = ~ 7e11 cm^{-2}) excitation regimes for PCE-10:$PC_{70}BM$ blends.

VI. References

1. Shrotriya, V.; Li, G.; Yao, Y.; Moriarty, T.; Emery, K.; Yang, Y., Accurate measurement and characterization of organic solar cells. *Adv. Funct. Mater.* **2006,** *16* (15), 2016-2023.
2. Kroeze, J. E.; Savenije, T. J.; Vermeulen, M. J. W.; Warman, J. M., Contactless determination of the photoconductivity action spectrum, exciton diffusion length, and charge separation efficiency in polythiophene-sensitized TiO2 bilayers. *J. Phys. Chem. B* **2003,** *107*, 7696-7705.
3. Ferguson, A. J.; Kopidakis, N.; Shaheen, S. E.; Rumbles, G., Dark carriers, trapping, and activation control of carrier recombination in neat P3HT and P3HT:PCBM blends. *J. Phys. Chem. C* **2011,** *115* (46), 23134–23148.
4. Dayal, S.; Kopidakis, N.; Rumbles, G., Photoinduced electron transfer in composites of conjugated polymers and dendrimers with branched colloidal nanoparticles. *Faraday Discuss* **2012,** *155*, 323-337.
5. Ye, L.; Zhang, S.; Zhao, W.; Yao, H.; Hou, J., Highly Efficient 2D-Conjugated Benzodithiophene-Based Photovoltaic Polymer with Linear Alkylthio Side Chain. *Chem. Mater.* **2014,** *26* (12), 3603-3605.